

AD-A257 623

2



NAVAL POSTGRADUATE SCHOOL Monterey, California



S DTIC
ELECTE
DEC 01 1992
D
E

THESIS

EMISSIVITY OF ROCKET PLUME PARTICULATES

by

CURTIS D. WHISMAN

SEPTEMBER 1992

Thesis Advisor:

DR. DAVID W. NETZER

92-30425

Approved for public release; distribution is unlimited

Approved for public release; distribution is unlimited

Emissivity of Rocket Plume Particulates

by

Curtis D. Whisman
Lieutenant, United States Navy
B.S., New School for Social Research, 1983

Submitted in partial fulfillment
of the requirements for the degree of

MASTER OF SCIENCE IN ASTRONAUTICAL ENGINEERING

from the

NAVAL POSTGRADUATE SCHOOL

September 1992

Author:

Curtis D. Whisman

Curtis D. Whisman

Approved by:

David W. Netzer

David W. Netzer, Thesis Advisor

Garth B. Hobson

Garth Hobson, Second Reader

Daniel J. Collins

Daniel J. Collins, Chairman

Department of Aeronautics and Astronautics

ABSTRACT

The optical properties of motor aluminum oxide are required inputs to current plume signature prediction codes, such as SIRRM. Accurate predictions are possible only if variations in the particle emissivity due to changes in particle size, contamination, and changing temperature, etc., are known.

This investigation demonstrated a simplified method for determination of the emissivity of rocket motor generated alumina. Plume particulate material was collected on tungsten alloy wire during motor firings. A DC circuit was used to resistively heat the material, and the temperature was determined at various points by relating the wire resistivity to circuit current and voltage. An Agema Thermovision infrared (3.5-5 μ) camera and microscope were used to observe the material during heating, and broad-band emissivity was computed using system software. It was estimated that the emissivity could be measured with an accuracy of $\pm 3\%$. Motor alumina was found to have significantly greater emissivity than pure alumina in the temperature range of 500-1200K.

DTIC QUALITY INSPECTED 2

Accession For	
NTIS CRA&I	<input checked="" type="checkbox"/>
DTIC TAB	<input type="checkbox"/>
Unannounced	<input type="checkbox"/>
Justification	
By	
Distribution /	
Availability Codes	
Dist	Avail and/or Special
A-1	

TABLE OF CONTENTS

I.	INTRODUCTION	1
II.	METHOD OF INVESTIGATION	10
III.	DESCRIPTION OF APPARATUS	11
IV.	EXPERIMENTAL PROCEDURE	25
V.	EXPERIMENTAL RESULTS	29
VI.	CONCLUSIONS AND RECOMMENDATIONS	32
	APPENDIX A. CATS-E SOFTWARE	34
	LIST OF REFERENCES	37
	INITIAL DISTRIBUTION LIST	38

LIST OF SYMBOLS

A	cross sectional area
c	speed of light, c/n
c_0	speed of light in a vacuum, 2.988×10^{10} cm/sec
h	Planck's constant, 6.625×10^{-27} erg sec
I	current, amps; Thermal Unit (Agema system)
k	Boltzmann's constant, 1.38×10^{-16} erg/K
l	length
n	index of refraction
S	black-body detected radiation, photons/sec
S'	attenuated object radiation, photons/sec
R	resistance, ohms
T, t	temperature, K
V	voltage, volts
W_b	spectral emissive power of a black-body, erg/sec cm^3
w_b	total emissive power of a black-body, erg/sec cm^2
α	absorptivity
ϵ	emissivity
λ	wavelength
ρ	reflectivity or resistivity
σ	Stefan-Boltzmann constant, 5.688×10^{-5} erg/sec $cm^2 K^4$
τ	transmissivity; Agema system correction factor

subscript

a	ambient
atm	atmosphere
bb	black-body
o	object
p	potentiometer
w	wire

I. INTRODUCTION

Analysis of solid propellant rocket motor exhaust plumes has been an ongoing and continuously evolving process for several decades. Of particular interest is the exact mechanisms by which combustion products, both gaseous and condensed, affect the radiation signature of the plume. As advancements in remote sensing technology have improved, the ability to model plume processes, predict performance, and accurately detect target platforms based on plume signature has not kept pace.

Significant levels of radiation are emitted from an exhaust plume over the entire electromagnetic (EM) spectrum. Emissions are particularly strong in the wavelength band from the infrared (IR) to the ultraviolet (UV) [Ref.1]. Most plume signature studies have concentrated on the IR portion of the EM spectrum. As materials technology advances, which reduce radar cross section, are assimilated into missile design an alternate method of identification, tracking, and targeting "hostiles" must be found. Despite our vast understanding of exhaust plume radiation characteristics, there is clearly incomplete knowledge of the particulate size distribution and optical properties in the plume.

Remote sensing of the radiation of a missile exhaust plume by passive detection techniques may prove to be an effective way to identify, track, and target a vehicle. Exhaust plume detection is possible by sensing either radiation emitted from the plume, or by detecting disturbances in the levels of ambient radiation [Ref.2].

The IR radiation data base currently used by plume prediction codes such as SIRRM, require additional input for variations in motor particulate emissivity. This parameter changes particle size, level of contamination, temperature, and other variables which may alter the optical properties of the particles.

The majority of particulate material in the exhaust plume of a metallized solid propellant motor consists of oxide particles produced during the combustion process. Powdered metals have been used extensively in conventional solid propellants. Metals are added to the propellant matrix to raise the specific impulse and thrust. Types of metals which have been used as fuels include aluminum, beryllium, magnesium, and zirconium [Ref.3].

The most widely used of these metal fuels is aluminum. It is readily available, low in cost, and has an acceptable density and heat of reaction. Aluminum fuel is most often added to the propellant matrix in the form of particles with diameters between five and 200 microns, with 10 to 40 microns being the most common size distribution. The mass fraction

generally varies between 12%-22%. Like all metals, aluminum is resistant to ignition and combustion because it does not vaporize at the temperature of the burning surface. This physical resistance to combustion is further aggravated by the tendency of molten aluminum to form large agglomerates on the burning surface. Formation of a "protective" oxide skin prolongs, and in some cases, prevents complete combustion of these large agglomerates [Ref.3].

For combustion of a particle or agglomerate to occur, the "droplet" must attain a temperature sufficient to melt and retract the oxide layer surrounding the molten aluminum core. Breakdown of the oxide skin initiates an oxidation reaction intense enough to induce a rapid thermodynamic temperature rise in the particle. At 1300K - 1500K, when exposed to oxidizing species in the combustion chamber, particle ignition will occur. The combustion temperature of the droplet stabilizes at approximately 2500K and is constrained on the low end by the melting temperature of the oxide, 2318K, and on the high end by the aluminum boiling point, 2750K. Below 2318K, surface oxide development will cause flame collapse, and at the metal boiling point the droplet will begin to vaporize, disrupting the droplet structure [Ref.4]. An equilibrium temperature of 2500K will sustain droplet combustion, while maintaining the integrity of the droplet structure [Ref.3].

The flame envelope surrounding a burning aluminum droplet contains a high concentration of molten aluminum oxide which condenses as it comes in contact with the cooler Ammonium Perchlorate (AP) combustion gases [Ref.3]. As burning of the droplet progresses, aluminum concentration in the droplet decreases, while the percentage of aluminum oxide, a by-product of the combustion process, increases [Ref.4]. As the aluminum is consumed, the surface aluminum oxide residue begins to dominate the combustion behavior of the droplet [Ref.3]. When aluminum concentration in the droplet is too low to support further combustion, the process ceases, and a core of molten aluminum oxide will remain [Ref.3].

Oxide particle size distribution in the combustion chamber is generally believed to be bi-modal. Flame generated "smoke" is approximately two microns in diameter, while the residue oxide droplets will generally be 5-50 microns after complete aluminum consumption. However, particles as large as several hundred microns in diameter can be present. It follows that the smaller the original agglomerate diameter and mass, the smaller the residue oxide droplet [Ref.3].

The presence of these residue aluminum oxide droplets and oxide "smoke" have a significant effect on the signature of the exhaust plume. Emission levels from the plume depend on the particle number density and size distribution. The level of radiation emission also depends upon the temperature and the particle optical properties, which can be affected by

particle contamination, size, and temperature [Ref.5]. Calculation of the contribution of aluminum oxide particles in the plume to the total plume emittance is complicated by the fact that, while "smoke" is believed to be mainly pure aluminum oxide, the larger particles are not pure aluminum oxide [Ref.6]. Studies by T.J. Reiger,[Ref.6], and A.B. Pluchino and D.E. Masturzo, [Ref.7], support the idea that the absorption coefficient of "motor alumina" is much greater than that for pure alumina (sapphire). The most widely accepted reason for this phenomenon is that the exhaust alumina is contaminated with another material [Ref.7]. Because solid propellant motors burn fuel rich, it may be possible that during the aluminum agglomerate combustion process that the particle may become contaminated with an excess fuel specie such as carbon [Ref.7]. It is also possible that as agglomerate residence time in the motor varies, larger agglomerates may not completely burn, leaving a small amount of aluminum in the final particle [Ref.6].

Theoretical and experimental studies performed by Rieger [Ref.6] in the two to five micron band of the infrared, found that as the volume percentage of metallic aluminum in the composite particle increased, there was a large increase in the total particle emissivity. It did not matter if the aluminum contamination was an outer shell, or a solid core.

Follow on studies to Riegers' work performed by Pluchino and Mastuzo [Ref.7] used the same model, but considered contamination of the composite particle by carbon. An aluminum oxide particle contaminated with carbon shows an absorption coefficient increase of one to three orders of magnitude over that of an uncontaminated particle [Ref.7].

Studies have shown that particle size and the crystal phase, either alpha or gamma, are properties that affect particle scattering characteristics. In general the smaller the particle the greater the scattering, and the smaller the particle emissivity [Ref.5]. These results seem to be consistent, regardless of the IR wavelength investigated [Ref.5].

Plume particulates scatter radiation emitted from other sources. The intensity of this radiation is dependant upon the radiation source, initial intensity, wavelength, particle scattering cross section, and the number density of the particles [Ref.1]. An example of this process is the "search light" effect. Radiation, originating in the combustion chamber, passes through the nozzle and is scattered by plume particulates. This gives the appearance that the light energy is originating in the plume. The higher the number density, all other factors being equal, the higher is this contribution to the plume radiation signature [Ref.2].

In addition to continuum emission by particles, IR emissions in the plume are also produced by the rotational-vibrational transitions in molecules. Results from spectral analyses of the plumes of conventional solid propellant motors show strong lines for H_2O , CO_2 , and CO [Ref.2].

The level of IR radiation that reaches a detector is also dependant upon the amount of plume emission attenuation during atmospheric propagation. Attenuation processes can include absorption and scattering by both particles and atmospheric molecular species such as CO_2 and H_2O [Ref.2].

While much data is available on the emissivity characteristics of pure alumina, there is little data available for contaminated motor aluminum oxide, and the data that does exist is usually wavelength and temperature specific. Plume codes, such as SIRRM, must perform considerable data extrapolation to arrive at numerical inputs applicable for further plume radiation predictions. To realistically predict plume signature the optical properties of the plume must first be accurately known. Depending upon propellant composition, combustion environment, and nozzle geometry, oxide particle properties can vary from motor to motor. A basic understanding of the effect that these motor variables have on particle properties (complex index of refraction, absorption coefficient, emissivity, etc) is needed.

A very reliable technique widely used to determine particle optical properties is laser ellipsometry. In this technique a target particle is illuminated with polarized laser light, and the level of scattered energy is determined by photo detectors placed at various locations around the particle. From the level of scattered energy the desired optical properties of the particle can be very accurately determined. The target particle is usually a large spherical particle, on the order of 500-1000 microns. Alumina particles present in the plume are typically much smaller than 200 microns in diameter, and the complex index of refraction varies widely with particle size [Ref.5]. Besides the utilization of a particle that is not necessarily a representative "average" of motor produced particles, the results are limited to the wavelength of the laser being used [Ref.8].

It would be most desirable to measure the particle's optical properties while it is present in the plume. Average emissivities, etc. can be determined in this manner, but the effects of particle size and contaminate levels are indeterminate. Thus, intrusive analysis techniques are generally used if specific results are desired. The particle collection method used should be as non-intrusive as possible to minimize the disruption to the plume flowfield, particle distribution, and particle size. The method must be repeatable, and provide a uniform sample of material.

To overcome the limitations imposed by current diagnostic techniques such as laser ellipsometry and spectroradiometry, this research sought to demonstrate a simplified technique for obtaining motor particulate optical properties as a function of motor/plume location, temperature and wavelength, over any desired wavelength band in the near to mid-IR. To achieve this objective, a reliable material collection method, a method for heating and accurately measuring the material temperature, and a device which could measure the emitted radiation in the near IR, were needed.

II. METHOD OF INVESTIGATION

In an attempt to demonstrate a reliable method for measuring the emissivity of motor alumina, a unique system has been devised. Pure tungsten wires, with known resistivity, are placed ^{at} ~~in~~ various locations in the plume or motor flowfield to collect condensed particulate material. The wire is then resistance heated to the desired temperature using a DC circuit. The wire is supported in the field of view of an infrared microscope and scanner system. IR images taken at each known temperature are then used to determine the emissivity of the oxide material.

III. DESCRIPTION OF APPARATUS

To determine the change in emissivity of motor aluminum oxide vs temperature, a method for heating the material to the desired temperature was required. Various methods of heating aluminum oxide particles have been used. Some of these methods include lasers, hydrogen\oxygen or propane\oxygen combustion systems, combustion bombs, and small scale-rocket motors. To meet the requirements of the present investigation, any heating method used must be capable of providing accurate control of temperature up through the melting point of aluminum oxide.

The initial method employed a hydrogen gas\air combustion system. The actual combustion chamber was a cylindrical jacket with a hollow tantalum tube passing through the center of the jacket. The tube provided a separation boundary and heat transfer path between the combustion gases and the sample air flow used to heat the particle. The particle was supported in the microscope field of view by a ceramic tube connected to a small vacuum system. The tube was mounted on an X,Y,Z translation stage which provided alignment in all three axes.

The system was designed to provide clean air flow, at a precisely controlled temperature, that would not contaminate the particle. Temperature control was achieved by varying the mass flow rate of the hydrogen gas into the system. However, rapid oxidation of the tantalum tube occurred at higher temperatures, resulting in tube failure after only a few runs. For this reason the heating method was abandoned.

The second heating method investigated used an AC resistive heating concept. Wire coils made from nichrome and platinum wire were inserted into zirconium ceramic tubes. An AC current was passed through the coils, resistively heating the sample air flow passing over the coils. This electrically heated air was directed onto the particle which was held in place by the same vacuum system discussed above. A high current potentiometer installed in the circuit provided temperature control by varying the current flow through the coils. Despite some difficulties with line current variations and potentiometer limitations, this method proved to be successful up to approximately 1400K.

As particle analysis progressed however, inconsistencies in particle emissivity calculations arose. Upon analyzing the procedure in detail, it was discovered that the problem was with the microscope thermal protection window. The IR microscope could be operated unprotected up to 473K. Beyond this point thermal protection must be provided to prevent damage to the optics. The window chosen was made of sapphire

which had good transmission qualities over the scanner operating bandwidth. Quartz has a varying attenuation in the IR bandwidth being utilized. It was discovered, however, that the transmission characteristics of the sapphire window changed as the temperature of the glass increased. Hot sample air incident on the glass during system operation, caused an unacceptable attenuation of the radiant energy reaching the scanner, resulting in the data irregularities noted. This technique was also abandoned and resulted in the termination of any individual particle work using a hot air heating system.

The system currently being used to determine the emissivity vs temperature characteristics of motor alumina is shown schematically in Figure 1. A simple series DC circuit was used to resistively heat a 0.51 mm diameter wire which had been coated with motor aluminum oxide.

Power for the circuit was provided by a 12 volt battery. A potentiometer was used to vary the voltage across the wire. The wire was positioned in the microscope field of view and connected in series in the circuit by two small clips mounted on an X,Y,Z translation stage. The stage was adjustable in all three axes, providing focusing capability.

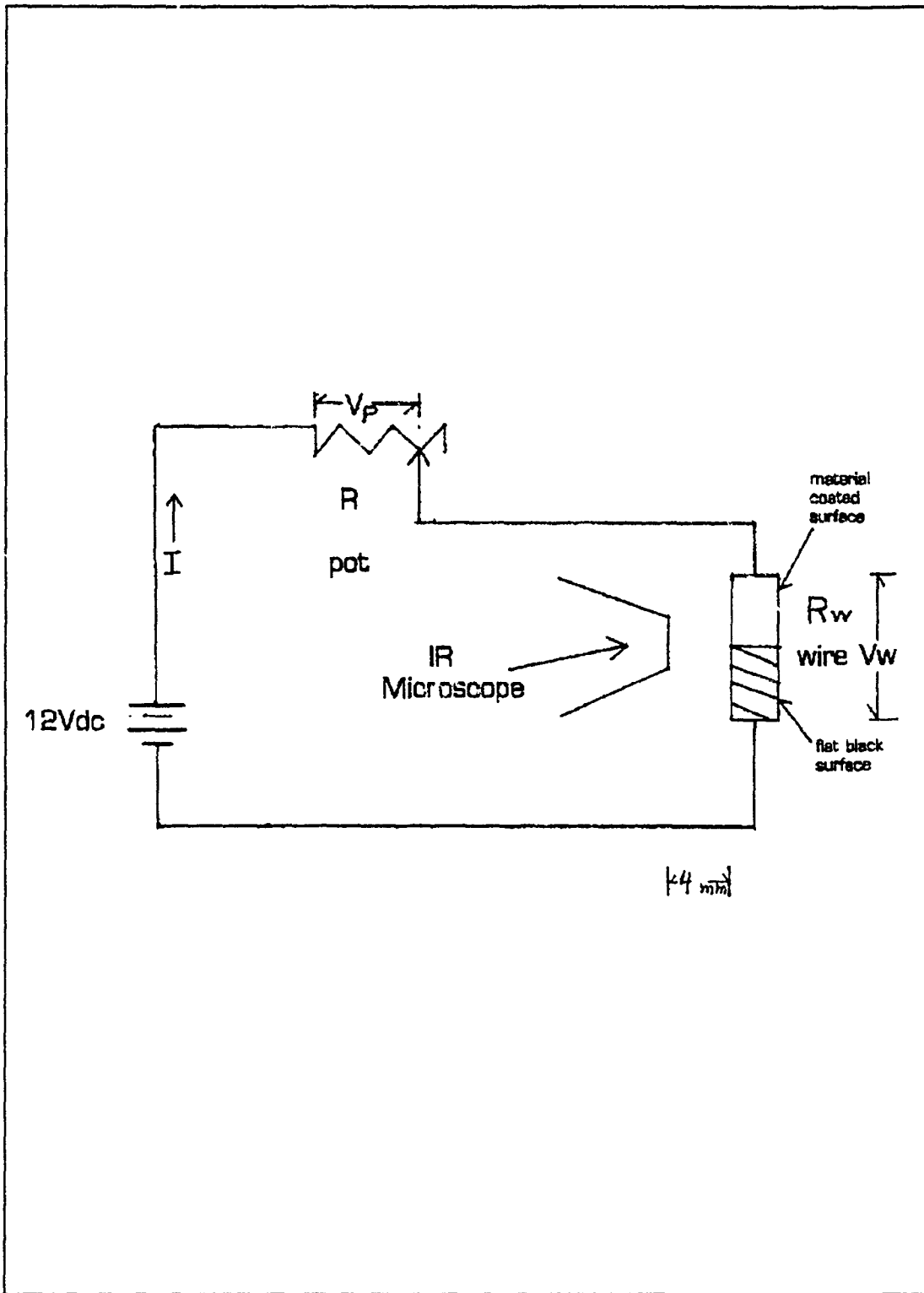


Figure 1 Experimental Circuit Schematic

Pieces of pure tungsten wire a few centimeters long can be placed in any desired location of an aluminized solid propellant motor during firing. Motor material will impinge on the wire, cool and solidify, forming a coating of motor alumina on the wire exterior. The high melting point of tungsten, 3683K, ensures that the wire will survive the combustion environment. Tungsten is also a very good electrical conductor, with an approximately linear variation in resistivity with temperature. The resistivity vs temperature of tungsten is shown in Figure 2.

The measurement system employed an Agema IR microscope and scanner. The Agema system uses an infrared detector that operates in the two to five micron spectral band. Supporting computer hardware and software make it possible to determine the temperature of an object, or by using a special menu function, determine the objects broad-band emissivity.

By definition black-bodies absorb all radiation incident upon them at all wavelengths. A black-body is equally capable of emitting all this incident radiation. Planck's law describes the radiation from a black-body at a specific wavelength and temperature, and is given by [Ref.10]:

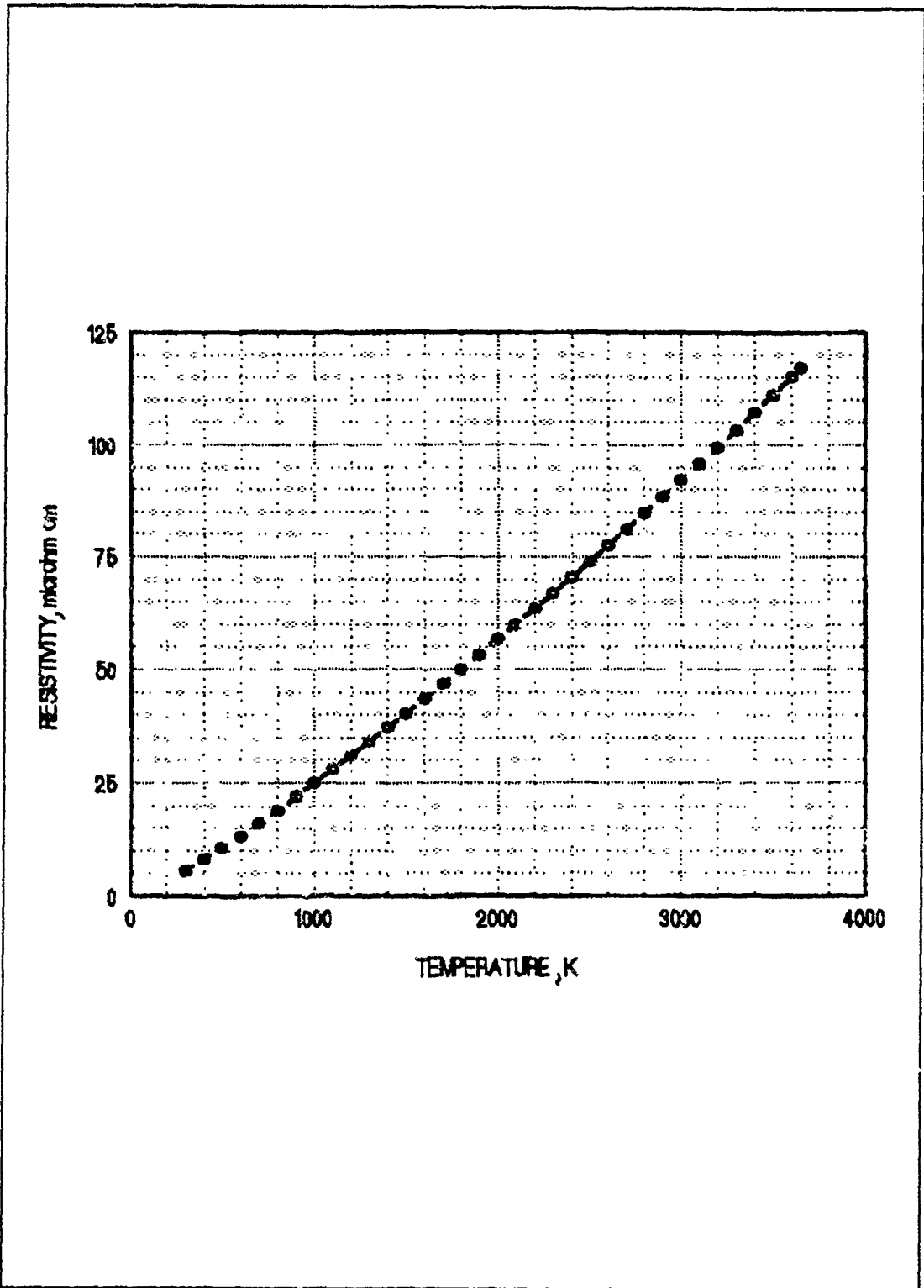


Figure 2 Pure Tungsten Wire Resistivity vs. Temperature

$$W_b = \frac{2\pi hc^2}{\lambda^5 \exp\left[\frac{hc}{\lambda kT}\right]}$$

Plotting Planck's Law for various temperatures and wavelengths produces a family of curves depicting spectral radiant emittance vs. wavelength. Each curve has a maximum value that is arrived at by differentiating Planck's Law.

If Planck's Law is integrated, the total radiant emittance of a black-body can be determined. This is the Stefan-Boltzman law and is given by:

$$W_b = \sigma T^4.$$

This equation states that total emission power from a black-body is proportional to the absolute temperature of the body, raised to the fourth power. Graphically the law represents the area under the Planck's curve at any specific temperature. [Ref.10]

Most objects are considered "gray-bodies" instead of pure absorbers or pure reflectors [Ref.10]. Three distinct electromagnetic processes occur in a gray-body that separate it from the characteristics of the black-body [Ref.10]. A portion of the radiation incident on the surface of a gray-body will be absorbed, some will be reflected, and some will

be transmitted. At any wavelength, the fractional portion of each process must sum to one at that wavelength. This relationship is given by [Ref.10]:

$$\alpha_{\lambda} + \rho_{\lambda} + \tau_{\lambda} = 1.$$

For opaque bodies $\tau_{\lambda} = 0$.

Emissivity is used to describe the ratio of the energy radiated by a gray-body as compared to that radiated by a black-body at the same wavelength and temperature. The spectral emissivity of a body is given by [Ref.10]:

$$\epsilon_{\lambda} = \frac{W_{\lambda}}{W_{\lambda_{bb}}}$$

Kirchhoff's law states that at any given wavelength the absorptivity equals the emissivity. For opaque materials, this implies:

$$\epsilon_{\lambda} + \rho_{\lambda} = 1.$$

These relationships provide the basis for the technology of IR detectors. While it is very difficult to measure the absorptivity of a material, the emittance is directly observable and measurable. If the emissivity of a body is taken into account, the power of a gray-body is the same as that of a black-body at the same temperature and wavelength,

While it is very difficult to measure the absorbtivity of a material, the emittance is directly observable and measurable. If the emissivity of a body is taken into account, the power of a gray-body is the same as that of a black-body at the same temperature and wavelength, reduced proportionally by the value of the emissivity. This is given by[Ref.10]:

$$W_g = \sigma \epsilon T^4 .$$

IR detectors utilize two different technologies to detect IR radiation. The first is the thermal detector which is sensitive to temperature changes of the body being analyzed. The second category of detectors are the quantum or photon detectors. In this type of IR detector, a semiconductor is used as the radiation sensitive medium. The semiconductor will release a specific number density of electrons proportional to the energy level of the incident photon "stream". The higher the energy of the photon, the larger the number of electrons released. This type of detector is very sensitive to wavelength changes in the incident radiation, and has very good response time characteristics. The resolution is not as good as in the thermal detector, however, because there is a minimum photon energy level below which no electron release from the semiconductor will occur.[Ref.10]

The IR detector used in this experiment was the Thermovision 870 photon detector produced by Agema corporation. The details of system operation can be found in Reference 10. Photon emissions from the object being viewed pass through the ambient environment that exists between the object and the scanner. The system takes the incident photon level and through the application of correction factors for atmospheric and object surrounding effects, computes a numerical value of spectral radiance from the object being viewed. Numerical values of object emissivity, atmospheric temperature, ambient surrounding temperature and distance between the object and the scanner are required system inputs to compute the object temperature. The algorithm the system uses to compute spectral radiance is given by:

$$\dot{S}_o = \tau_o \epsilon_o S_o + \tau_o (1 - \epsilon_o) S_a + (1 - \tau_o) S_{atm}.$$

The first term on the right hand side of the equation is the object emitted radiation. The second term is reflected radiation from the object surroundings, and the third term represents atmospheric radiation effects. [Ref.10] This is represented in Figure 3.

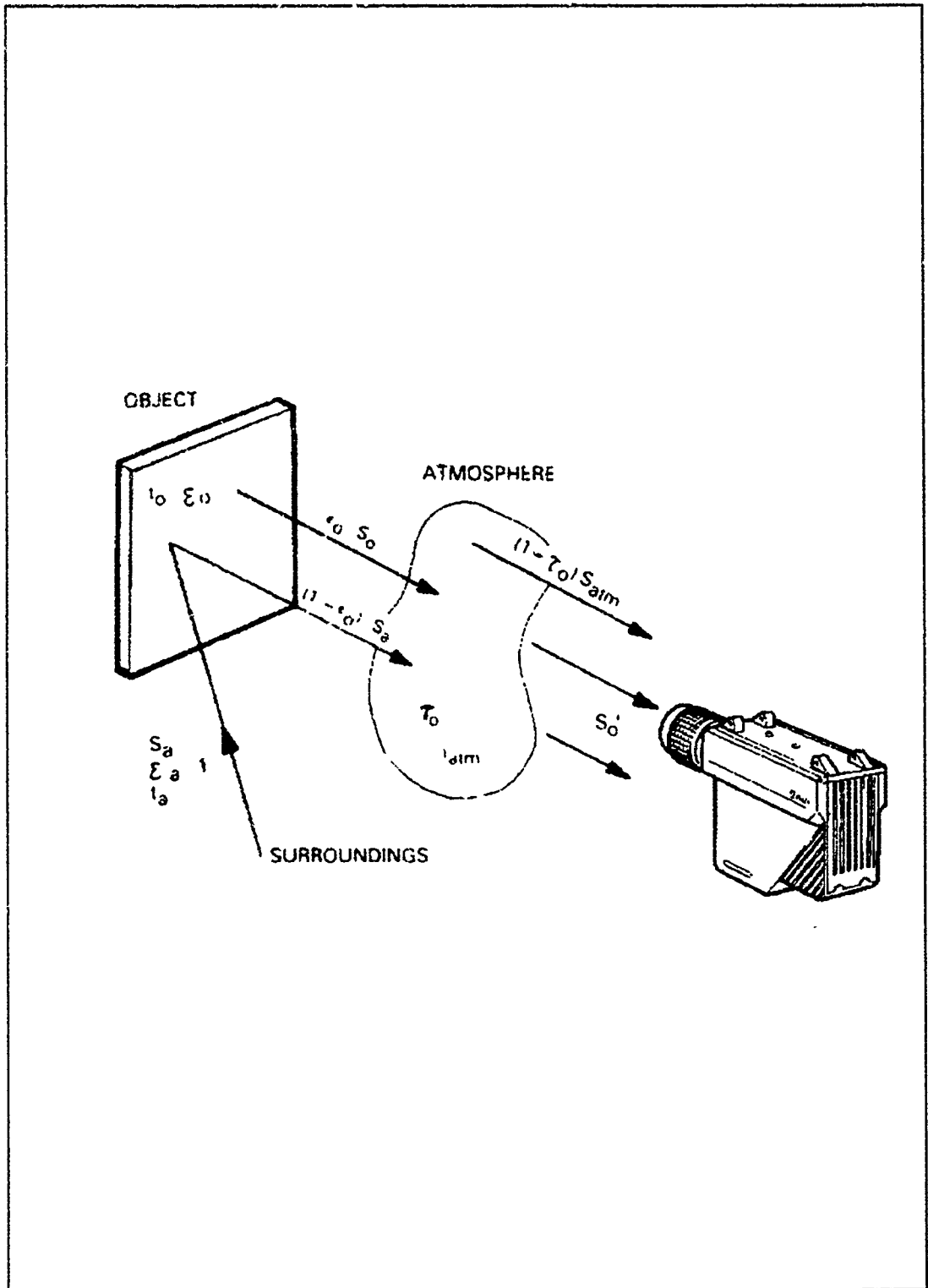


Figure 3 Agema IR Scanner Theory of Operation (Ref.10)

Using the linear relationship between the instrument calibration and the received photon energy, the system computes an arbitrary unit called a "thermal unit", I, to represent the displayed spectral emittance. The general formula, expressed in terms of thermal units, used by the system to produce the digital visual display is given by:

$$\dot{I}_o = \tau_o \epsilon_o I_o + \tau_o (1 - \epsilon_o) I_a + (1 - \tau_o) I_{atm}$$

This formula represents the radiant power received by the detector from the object of interest, corrected for emittance from the object environment. [Ref.10]

If, however, the object temperature is known, but the emissivity is not, the system has a built in function called ECALC which will compute the object emissivity. It was this function that was used in this investigation to determine emissivity vs temperature changes of "motor" aluminum oxide. For the ECALC function to accurately compute object emissivity, the temperature of the object must be known.

Viewing a 0.51 mm diameter piece of motor oxide coated tungsten wire requires some type of optical magnifying system. For this project the Agema microscope was used in conjunction with the Thermovision 870 scanner. The scanner/microscope are interfaced through the CATS E Thermal Analysis software, which is MS-DOS based, and can be run on any 286 or higher CPU. This system allows real-time imagery of small objects such as alumina particles, with good optical resolution and thermal sensitivity.

Two filters were used with the system to provide some wavelength band versatility. Position 0 utilizes no filter and allows analysis over the band from 2 to 5 microns. The glass filter, setting 1, covers the band from 3.5 to 5 microns. The flame filter, setting 2, is a narrow bandpass filter with a peak at 3.85 microns.

The versatility of the system allows the scanner and microscope to be mounted in a vertical or horizontal position as required for the particular application. To facilitate placement of system components, the scanner and microscope were mounted horizontally. At setup, the microscope software is calibrated using a black-body source to establish the parameters required by the CATS program for proper microscope/scanner interface. A complete description of microscope calibration, setup, and operation is covered in detail in the Agema IR Microscope Manual [Ref.10].

To ensure proper operation of the system, the CATS E software has numerous menus and functions to choose from. For convenience and procedural efficiency, the functions applicable to this particular experimental investigation are summarized in Appendix A.

Some important system operation requirements are worth mentioning. LIDAT is the menu selection which interfaces between the operator and the software package. It is in LIDAT that background emissivity, ambient surrounding temperature, and atmospheric temperature are entered. The object distance parameter should always be set to 0.6 m, the aperture set to zero, and M16 entered in the lens parameter when the microscope is to be used as recommended by Reference 10. These inputs are required for proper interface between all system components, and ensures that the emissivity algorithm computes the proper correction factors to account for atmospheric and environmental spectral effects.

IV. EXPERIMENTAL PROCEDURE

Validation of the system had to be performed using 0.51 mm diameter tungsten-rhenium alloy wire, (W-RE), due to the unavailability of pure tungsten wire. The resistivity characteristics of this wire were unknown, so a procedure had to be devised to determine the resistivity vs. temperature characteristics. A known length of the wire was painted flat black with a high temperature paint with an assumed emissivity of 0.95. The wire was then placed in the circuit and located at the focal distance of the Agema microscope. Initially the potentiometer was turned to the desired resistance setting while the circuit was de-energized. The circuit was then energized for five seconds, the image from the scanner frozen, and the voltages across the pot and wire recorded. Circuit resistances and voltages were measured using precision multimeters. A background emissivity reading of 0.95 for the black paint was entered in LIDAT, to determine the temperature of the wire from the program temperature scale. Wire resistance, R_w , was computed from pot resistance, R_p , pot voltage, V_p , and wire voltage, V_w , by the expression:

$$R_w = \frac{V_w}{V_p} R_p.$$

R_w was also computed, using a high current ammeter, by the expression:

$$R_w = \frac{V_w}{I}$$

Once R_w was computed for a series of increasing temperatures, (to the point limit of 810 K), the resistivity of the wire was computed by:

$$\rho = \frac{A_w}{L_w} R_w$$

It is important to note that resistivity is in microhms centimeter. To ensure that the calculations were as accurate as possible, all measurements were taken to four significant figures. A plot of temperature vs. resistivity of the W-Re wire is shown in Figure 4. An assumption was made that W-Re has linear resistance vs. temperature characteristics at higher temperatures. This was a reasonable assumption since 75% of the wire was tungsten. Using this assumption, an extrapolation of the resistivity curve was made above 811 K.

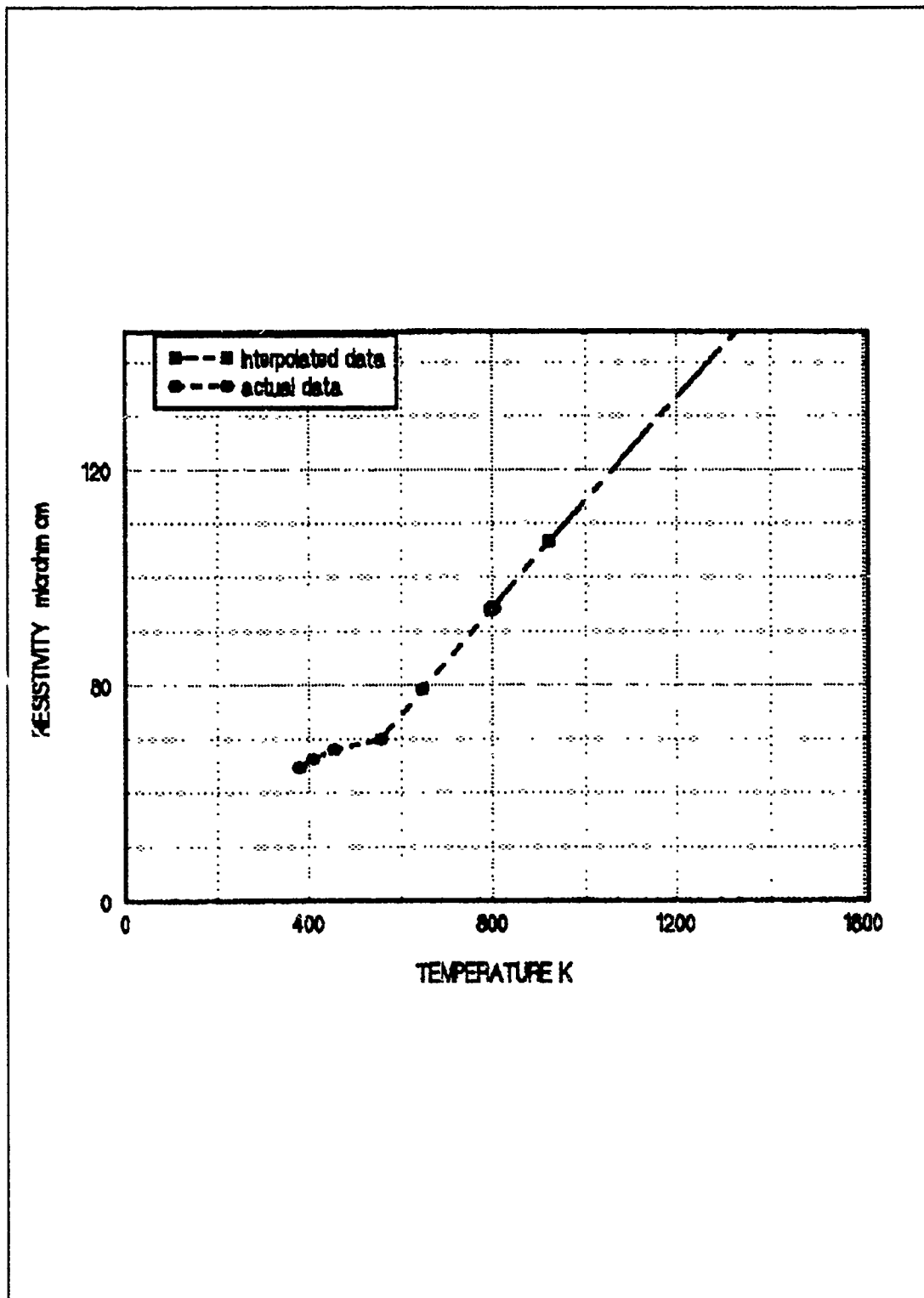


Figure 4 Tungsten-Rhenium Wire Resistivity vs. Temperature

Once the resistivity data was available, the wire was replaced with a motor alumina coated wire. The process was repeated, but this time the temperature was "known" and the emissivity was calculated. The resistance of the motor coated wire must be checked against that of a non-coated piece of the same length to verify that the connection points on the motor wire are clean. A microscope can also be used to verify that the circuit connection is made to bare wire. All measurements must be made as precisely as possible to ensure attainment accurate resistivity values.

It should be noted that the oxide coating needs to be relatively thick so that the measured emissivity is dominated by the coating. Composite materials, (in this case oxide on tungsten), radiate differently than pure material. A Mie code needs to be used to accurately predict the contribution of the tungsten wire as a function of oxide coating thickness. In any case, the relative effect of motor contaminates on emissivity can be assessed using this technique if a fixed coating thickness is utilized.

V. EXPERIMENTAL RESULTS

At the completion of the test run, the recorded data was used to compute the wire resistance and resistivity using the equations given previously, and the temperature at each point was taken from Figure 4. Each image was then recalled from storage, emissivity calculation areas created, and the emissivity in each area computed using the ECALC function. The temperature for each point from Figure 4 was used as the input to ECALC. Emissivity calculation areas were aligned along the wire centerline because the radiation along the center line was most normal to the plane of the microscope lens. The emissivity vs. temperature results are shown in Figure 5. Also shown for comparison are the emissivities of pure aluminum oxide, and pure tungsten. Although the tungsten may contribute to the measured emissivity as discussed above, it is apparent from Figure 5 that the motor alumina had significantly greater emissivity than pure alumina. The glass filter was used to ensure that the maximum system temperature range over the widest spectral band could be used. The Agema system was supposed to be calibrated to 2367K. However, it was found that the software limited the maximum temperature to 990K. Thus, the data could not be obtained through the desired melting temperature of aluminum oxide, 2318K.

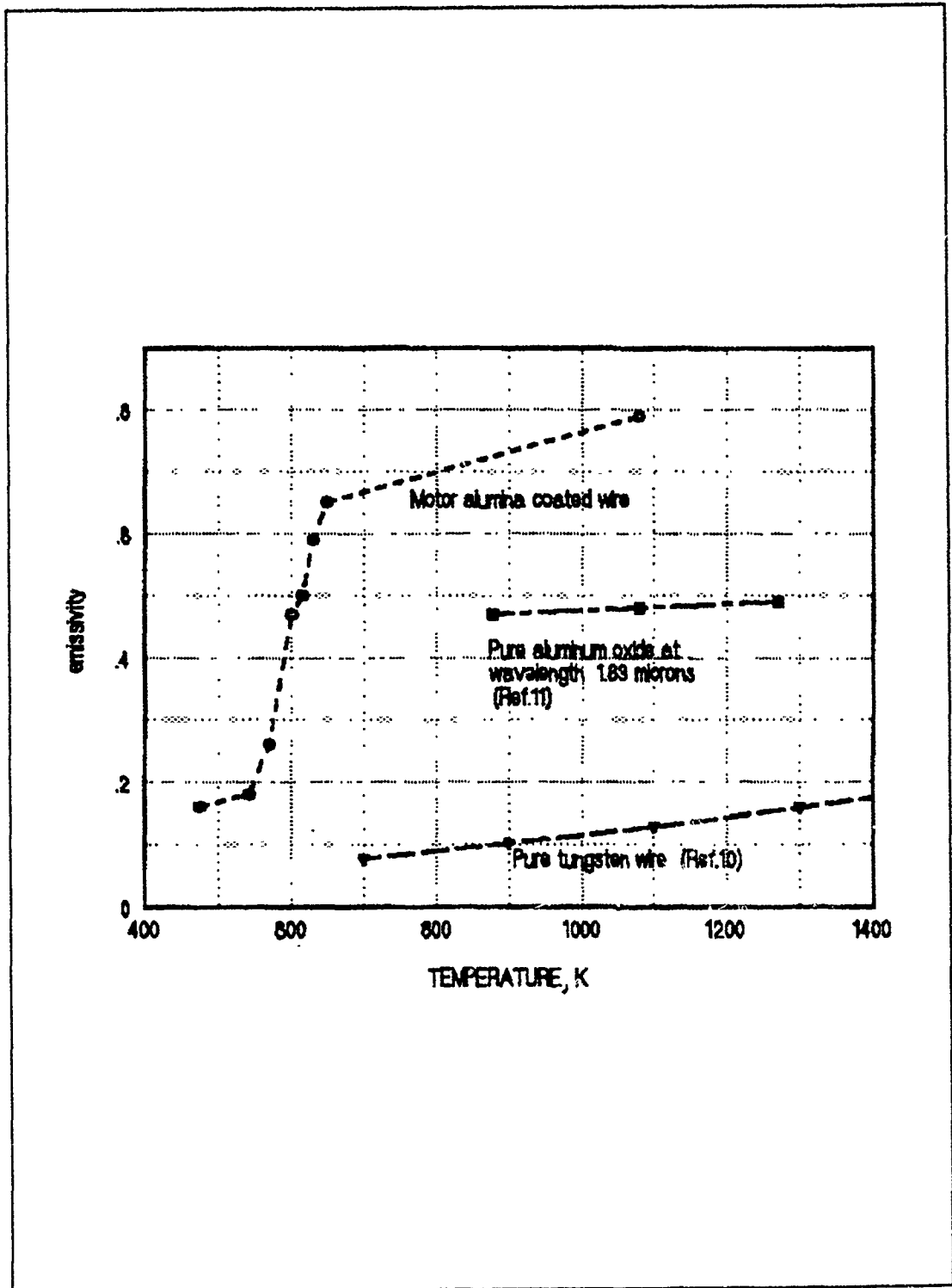


Figure 5 Emissivity vs. Temperature of Motor Alumina taken during System Validation Test Run

The uncertainties in V , V_w , R , and I were approximately $\pm 2\%$. Using the measured V_w and I for obtaining R_w results in an uncertainty in R_w of $\pm .2\%$ at elevated temperatures. This results in an uncertainty in the calculated temperature of ± 3 K. This small variations in temperature does not change the value of emissivity determined by the Agema system. Thus, the only significant uncertainty in the measured emissivity is due to the Agema camera and software. The accuracy of the Agema system for determining the emissivity for a specific temperature is unknown. However, the emissivity is displayed to two significant figures. If this is taken as the system accuracy, at low emissivities, (ie. 0.20), this would yield an emissivity of approximately $\pm 3\%$.

VI. CONCLUSIONS AND RECOMMENDATIONS

This investigation has demonstrated a new method for measuring the emissivity of rocket motor generated aluminum oxide. Pure tungsten wire is coated by placement in the desired location of the motor or plume, and then resistively heated under an IR microscope. The estimated accuracy of the measured emissivity is $\pm 3\%$. Circuit improvements such as a larger battery and a high power potentiometer with more precise control at lower resistance settings should improve the operational accuracy of the system. An automatic data recording system with an external sequential trigger should be used to replace the current manual method of data acquisition.

A method to more uniformly coat the Tungsten wire should be used, such as rotating the wire during firing. A uniformly coated wire will make microscope focusing and emissivity calculation area placement much more consistent. The effects of coating thickness on the contribution of the tungsten to the measured emissivity needs to be determined. If a viewing protection window for the microscope can be found that does not change transmission characteristics with temperature, measurements using large single motor alumina particles could once again be attempted. The single particles eliminate the problem of having composite materials present.

Preliminary data suggests that broad-band emissivity of motor alumina increases with increasing temperature, and is significantly greater than that of pure alumina. Once scanner calibration is complete, and mechanical improvements to the circuit are made, the repeatability of the procedure must be demonstrated. When higher temperatures can be observed, some very useful emissivity data should be obtained. This data will be very useful in validating the data base currently used in SIRR, and for investigating the effects of contaminants/additives on the optical properties of aluminum oxide.

Preliminary data suggests that broad-band emissivity of motor alumina increases with increasing temperature, and is significantly greater than that of pure alumina. Once scanner calibration is complete, and mechanical improvements to the circuit are made, the repeatability of the procedure must be demonstrated. When higher temperatures can be observed, some very useful emissivity data should be obtained. This data will be very useful in validating the data base currently used in SIRR, and for investigating the effects of contaminants/additives on the optical properties of aluminum oxide.

CAL: Lists the calibration data R,B, and F for each aperture and lens.

SIDAT: The still image equivalent to LIDAT.

CREA: Creates an analysis area on the image. Default shapes can be selected, or a custom area shape can be created. The area should be placed in a position of uniform color when using it to perform emissivity calculations. CTRL arrow keys change the area size, arrow keys alone move the area in the X,Y plane. To perform an emissivity calculation an area must be created.

ICOMP: Used to select the number of pixel scans performed by the SHINT function to compute emissivity. The higher the number of scans, the longer the calculation takes.

SHINT: Performs a pixel averaging function which smooths out variations in the digital image.

STAT: Statistical function command that is used before the ECALC command. The averaging function is being performed on the selected area.

CAL: Lists the calibration data R,B, and F for each aperture and lens.

SIDAT: The still image equivalent to LIDAT.

CREA: Creates an analysis area on the image. Default shapes can be selected, or a custom area shape can be created. The area should be placed in a position of uniform color when using it to perform emissivity calculations. CTRL arrow keys change the area size, arrow keys alone move the area in the X,Y plane. To perform an emissivity calculation an area must be created.

ICOMP: Used to select the number of pixel scans performed by the SHINT function to compute emissivity. The higher the number of scans, the longer the calculation takes.

SHINT: Performs a pixel averaging function which smooths out variations in the digital image.

STAT: Statistical function command that is used before the ECALC command. The averaging function is being performed on the selected area.

LIST OF REFERENCES

1. Bartky, C.D. and Bauer, E., "Predicting the Emittance of a Homogeneous Plume Containing Aluminum Particles", Journal of Spacecraft and Rockets, V.3, No.10, pp. 1523-1526, 1966.
2. Victor, A.C., "Plume Considerations", To appear in a forthcoming AIAA Volume on Tactical Missile Propulsion, pp. 1-29.
3. Price, W.E., "Combustion of Metalized Propellants", Fundamentals of Solid Propellant Combustion, Progress in Astronautics and Aeronautics Series, V.90, pp. 479-513, 1984.
4. Brewster, M.Q., "Radiative Properties of Burning Aluminum Droplets", Combustion and Flame, V.72, pp. 287-299, 1988.
5. Nelson, H.F., "Influence of Scattering on Infrared Signatures of Rocket Plumes", Journal of Spacecraft and Rockets, V.21, No.5, pp. 425-432, 1984.
6. Rieger, T.J., "On the Emissivity of Alumina/Aluminum Composite Particles", Journal of Spacecraft and Rockets, V.16, No.16, pp. 438 and 439, 1979.
7. Masturzo, D.E. and Pluchino, A.B., "Emissivity of Aluminum Oxide Particles in a Rocket Plume", American Institute of Aeronautics and Astronautics Journal, V.19, pp. 1234-1236, 1981.
8. Mularz, E.J. and Yuen, M.C., "An Experimental Investigation of Radiative Properties of Aluminum Oxide Particles", Radiant Transfer, V. 12, pp. 1553-1568, 1972.
9. Handbook of Chemistry and Physics, 68th ed., p. E406, CRC Press, 1987.
10. Agema Infrared Systems, "Thermovision 870 Operating Manual", Sects. 8 and 9, 1986.
11. Thermodynamic Properties of Selected Aerospace Materials, Thermal Radiative Properties, Part 1, pp. 250-252, Thermophysical and Electronics Properties Information Center, Purdue University, 1976.

INITIAL DISTRIBUTION LIST

	No. Copies
1. Defence Department Information Center Cameron Station Alexandria, VA 22304-6145	2
2. Library, Code 0142 Naval Postgraduate School Monterey, CA 93943-5002	2
3. Department Chairman, Code AA Department of Aeronautics and Astronautics Naval Postgraduate School Monterey, CA 93943-5002	1
4. Professor D.W. Netzer, Code AA/Nt Department of Aeronautics and Astronautics Naval Postgraduate School Monterey, CA 93943-5002	2
5. LT. Curtis D. Whisman 19050 Stratford Rd. #111 Minnetonka, MN 55345	2